



Contribution of precipitation events with different consecutive days to summer rainfall change over China

Ting You^{1,2} · Renguang Wu^{1,3,4} · Ge Liu⁵ · Zhaoyang Chai^{2,6}

Received: 2 December 2019 / Accepted: 1 June 2020 / Published online: 13 June 2020
© Springer-Verlag GmbH Austria, part of Springer Nature 2020

Abstract

The climatological features, regional trends, and interdecadal changes of summer precipitation over China are investigated in this study from the perspective of four types of precipitation events with different consecutive days. The precipitation events are classified based on the consecutive days of precipitation into 1-to-3-, 4-to-7-, 8-to-14-, and over-14-day events. The contribution of 1-to-3-day events to climatological precipitation is larger than the other events over central Asia. Longer duration events contributed more than the shorter duration events to precipitation in tropical regions. The positive precipitation trend in northwestern and southern China is mainly due to 4-to-7-day and 8-to-14-day events, respectively; and the negative precipitation trend in North China is largely related to 4-to-7-day events. In general, the frequency change of precipitation events is a major reason for the precipitation change of these events in the concerned regions. The precipitation decrease in northern China around the mid-1960s is attributed to the reduction in 4-to-7-day events. The precipitation increase in northeastern and central China in the late 1970s is due to a combination of increases in 4-to-7-day and 8-to-14-day events. The precipitation increase in southern China around 1993 is mainly contributed by over-14-day events. The precipitation decrease in the mid-latitude Asia is due to the decrease in 4-to-7-day events. Most of the interdecadal precipitation changes are related to decrease or increase in the activity of anomalous cyclones. Results suggest that the frequency of occurrence of cyclonic perturbations is a major factor for interdecadal changes in summer precipitation over China.

Keywords Types of precipitation events · Summer precipitation trends · Interdecadal changes · Frequency of precipitation events

1 Introduction

Precipitation is a vital component of the water cycle, and it is the main source of local water resources. During the recent decades, great efforts have been made to investigate the trends in total precipitation amount and in the amount and frequency of precipitation with different intensities, such as light, moderate, and heavy precipitation as well as in absolute and relative precipitation extremes in the global land (Wen et al. 2015; Nguyen et al. 2018) and national regions (Karl and Knight 1998; Liu et al. 2005; Qian and Lin 2005; Zhai et al. 2005; Ding et al. 2007; Malik et al. 2016). In China, summer precipitation decreased in North China and Northeast China and increased in the Yangtze River regions, coastal South China, and northwestern China since the early 1950s (Liu et al. 2005; Zhai et al. 2005; Ding et al. 2007; Lu et al. 2014). Extreme precipitation events with long duration and strong intensity can cause large economic and societal losses in China (Yan 1998; Zong and Chen 2000; Yuan et al. 2012). Thus, it is important to understand the spatial and temporal variations

✉ Renguang Wu
renguang@zju.edu.cn

¹ Center for Monsoon System Research, Institute of Atmospheric Physics, Chinese Academy of Sciences, Beijing, China

² College of Earth and Planetary Sciences, University of Chinese Academy of Sciences, Beijing, China

³ Department of Atmospheric Sciences, School of Earth Sciences, Zhejiang University, 38 Zheda Road, Xihu District, Hangzhou 310027, China

⁴ State Key Laboratory of Numerical Modeling for Atmospheric Sciences and Geophysical Fluid Dynamics, Institute of Atmospheric Physics, Chinese Academy of Sciences, Beijing, China

⁵ Institute of Climate System, Chinese Academy of Meteorological Sciences, Beijing, China

⁶ International Center for Climate and Environment Sciences, Institute of Atmospheric Physics, Chinese Academy of Sciences, Beijing, China

of different types of precipitation events and their contributions to long-term changes in total precipitation.

The interdecadal variability of summer precipitation in China has been studied by previous studies (Yan et al. 1990; Gong and Wang 2000; Ding et al. 2008; Yao et al. 2008; Wu et al. 2010; Zhu et al. 2010; Huang et al. 2011; Liu et al. 2011; Huang et al. 2012; Liu and Wu 2016). Four major interdecadal changes have been identified, which occurred around the mid-1960s, late 1970s, early 1990s, and late 1990s. Yan et al. (1990) indicated a decrease in summer rainfall in North China around the mid-1960s. Gong and Wang (2000) showed that mean precipitation in eastern China has been above normal since the late 1970s. Ding et al. (2008) found that the summer precipitation in eastern China is characterized by more precipitation in North and Northeast China during 1951–1978, a southward shift of more precipitation band to the Yangtze River basin during 1978–1992 and further extension of more precipitation region to southern China during 1993–2004. The summer rainfall in North China and Northeast China displays a notable decrease around 1999 (Liu et al. 2011; Huang et al. 2012).

The frequency and intensity of precipitation are as vital as the amount of precipitation (Trenberth 2011). Most of the previous studies are mainly concerned with the intensity and frequency in the investigation of changes in precipitation characteristics. Several studies considered the temporal duration of precipitation events (Zolina et al. 2005; Zolina et al. 2010; Huang et al. 2011; Zolina et al. 2013; Zolina 2014; Liu and Wu 2016). Zolina et al. (2010) showed that wet spells (consequent days with significant precipitation) have become longer over most of Europe by about 15–20% during the period 1950–2008. Huang et al. (2011) analyzed the linear trends of different durations of continuous Meiyu precipitation and found that longer-duration precipitation has become significantly less frequent since 2000, while 2-day and 3-to-4-day continuous precipitation processes have become more frequent. The longer duration of precipitation events is related to the slower progression of planetary waves in 500-hPa height fields, which would result in more persistent weather patterns (Francis and Vavrus 2012; Screen and Simmonds 2014; Guilbert et al. 2015). Long extreme precipitation events (3–10 days) in Ore Mountains may mainly be related to either slow-moving cut-off low or strong zonal circulation when many successive cyclones from west/northwestern cross over the area (Minářová et al. 2017). From August 23 to 25, 2004, Typhoon Aere affected Taiwan for 3 days (CWB, 2004). Trepanier and Tucker (2018) found that tropical cyclone rainfall in Houston, Texas and Miami, Florida last fewer than 4 days. The largest accumulations of precipitation in subtropical/mid-latitude locations may result from successive frontal systems over multiple days (Norris et al. 2019). These previous studies suggest that different precipitation lifetimes are associated with different types of atmospheric circulation systems.

Although many papers have documented changes in the frequency and intensity of precipitation events in China, few studies have analyzed precipitation events with multiple day duration. Understanding changes in the duration of precipitation days, as well as changes in the frequency and intensity of precipitation and their relationships to changes in the amount of seasonal precipitation, can be helpful in revealing the main factors of changes in precipitation amount. Distinct from most previous studies, we classify the precipitation events based on the duration of consecutive days and examine the changes in frequency, intensity, and duration of precipitation events with different consecutive days and their respective contributions to total summer precipitation amount changes in China in this paper.

The objectives of this study are to quantify the contributions of different precipitation events to summer precipitation amount changes and analyze which characters (intensity, duration, and frequency) account for the changes in the amount of precipitation for different precipitation events. The rest of the paper is organized as follows. Section 2 describes the data and methods used. In Section 3, we present the climatological characteristics of four types of precipitation events during the summer season (June–July–August) during 1951–2015. Contributions of intensity, duration, and frequency of precipitation events to long-term tendencies of summer precipitation are analyzed in Section 4. In Section 5, we document the contributions of intensity, duration and frequency of precipitation events to the interdecadal changes of summer precipitation. Section 6 presents a summary of the present study.

2 Data and methods

2.1 Data

In this study, the daily precipitation dataset was obtained from the Asian Precipitation-Highly Resolved Observational Data Integration Towards Evaluation of Water Resources (APHRODITE) (Yatagai et al. 2012). The time period for this dataset is from 1951 to 2015. This dataset is subject to strict quality control procedures and has been used in numerous studies (Yatagai et al. 2012; Lutz et al. 2014; Liu et al. 2016; Liu and Wu 2016). An angular distance averaging with a Sheremap-type scheme was used to obtain the gridded precipitation data. For details of the procedure, please refer to Yatagai et al. (2012). The number of gauges that passed the quality control increases gradually during the 1950s and 1960s. In the monsoon Asian region that is the focus of the present analysis, the number of gauges that passed the quality control is quite large starting 1951 and even there is more number of gauges in the 1950s than in the early 1970s (see Fig. 3 of Yatagai et al. 2012).

The daily output from the National Centers for Environmental Prediction-National Center for Atmospheric Research (NCEP-NCAR) Reanalysis (Kalnay et al. 1996) for the period 1951–2015 and from the European Center for Medium-Range Weather Forecasts interim reanalysis (ERA-Interim) (Dee et al. 2011) for the period 1979–2015 were used to examine changes in circulation features. The locations of the storms were based on the Joint Typhoon Warning Center (JTWC) “best-track” database (Knapp et al. 2010).

2.2 Methods

2.2.1 Classification of precipitation events

Following Liu and Wu (2016), the precipitation events are classified into four types based on the number of consecutive days with the daily precipitation amount exceeding 1 mm/day: 1–3 days, 4–7 days, 8–14 days, and over 14 days. This classification is based on the reasoning that precipitation in a certain region with different consecutive days is induced by the circulation systems that have a different life span. Here, we show two examples to illustrate the dependence of the length of precipitation event on the circulation system.

One example is a short precipitation event due to the tropical synoptic system. On October 12–14, 1995, a typhoon affected southern China, leading to a precipitation event there with 3 days (October 12–14) (Fig. 1g). The variation of rainfall amount is consistent with the movement of the typhoon (Fig. 1a–f). Large precipitation is observed when the typhoon approached the coast of South China (Fig. 1a–d). The precipitation amount is reduced after the typhoon dissipated (Fig. 1d–f). The other example is a precipitation event over southern China lasting 5 days. A low system developed over the eastern Tibetan Plateau and moved eastward during June 12–15, 1995 (Fig. 2a–d). When the low system arrived at southeastern China, the associated southwesterly lower-level winds induced large precipitation over southern China (Fig. 2c–f). Meanwhile, another low system was sustained over the eastern Tibetan Plateau (Fig. 2d–h), and it finally moved quickly eastward to eastern China (Fig. 2i). During the process, the subtropical high was maintained over the western North Pacific. The subtropical high and the eastward-moving low systems together resulted in the 5-day precipitation event from June 14 to June 18, 1995, over southern China (Fig. 2j). The above examples reveal that different precipitation durations over a certain region are affected by different circulation systems. Thus, it is meaningful to classify precipitation events based on the consecutive days of precipitation.

2.2.2 Three factors of precipitation events

The total rainfall amount of a precipitation event (PE) depends upon intensity, duration, and frequency. Following Dairaku

et al. (2004), for a PE in the year j , the relationship of rainfall amount to intensity and duration relationship is as follows:

$$R_{k,j} = I_{k,j}D_{k,j} \tag{1}$$

where $R_{k,j}$ represents the rainfall amount of the k th event in the year j , $I_{k,j}$ represents the intensity of the rainfall event k in the year j , and $D_{k,j}$ represents the duration of the rainfall event k in the year j . The total summer rainfall amount of the year j is represented by

$$\sum_0^{N_j} R_{k,j} = \sum_0^{N_j} I_{k,j}D_{k,j} \tag{2}$$

The mean rainfall intensity is defined as

$$\bar{I}_j = \frac{\sum_0^{N_j} R_{k,j}}{\sum_0^{N_j} D_{k,j}} = \frac{\sum_0^{N_j} I_{k,j}D_{k,j}}{\sum_0^{N_j} D_{k,j}} \tag{3}$$

Here, $\sum_0^{N_j} D_{k,j}$ is the total rainfall duration of PE in the year j . The average duration of the PE is defined by

$$\bar{D}_j = \frac{1}{N_j} \sum_0^{N_j} D_{k,j} \tag{4}$$

where N_j represents the number (or frequency) of PE in the year j .

The total rainfall amount of a PE is related to three factors: mean rainfall intensity, average rainfall duration, and frequency. The resultant equation is as follows:

$$\sum_0^{N_j} R_{k,j} = \sum_0^{N_j} I_{k,j}D_{k,j} = \frac{\sum_0^{N_j} I_{k,j}D_{k,j}}{\sum_0^{N_j} D_{k,j}} \frac{\sum_0^{N_j} D_{k,j}}{N_j} N_j \tag{5}$$

The frequency is defined as the number of events that occurred with the daily precipitation greater than 1 mm/day. The intensity is defined as the mean amount of precipitation during each day in which precipitation events occurred. Following Liu and Wu (2016), the duration of a rainfall event is defined as the number of days with consecutive precipitation over 1 mm/day.

The total amount of summer precipitation P_j in the year j is calculated by

$$\begin{aligned} P_j &= P_{j,1-3\text{day}} + P_{j,4-7\text{day}} + P_{j,8-14\text{day}} + P_{j,14+\text{day}} \\ &= \bar{I}_{j,1-3\text{day}} \bar{D}_{j,1-3\text{day}} N_{j,1-3\text{day}} \\ &\quad + \bar{I}_{j,4-7\text{day}} \bar{D}_{j,4-7\text{day}} N_{j,4-7\text{day}} \\ &\quad + \bar{I}_{j,8-14\text{day}} \bar{D}_{j,8-14\text{day}} N_{j,8-14\text{day}} \\ &\quad + \bar{I}_{j,14+\text{day}} \bar{D}_{j,14+\text{day}} N_{j,14+\text{day}} \end{aligned} \tag{6}$$

where $P_{j,1-3\text{day}}$, $P_{j,4-7\text{day}}$, $P_{j,8-14\text{day}}$, and $P_{j,14+\text{day}}$ are the amount of precipitation of the 1-to-3-day, 4-to-7-day, 8-to-14-day, and over-14-day events in year j , respectively.

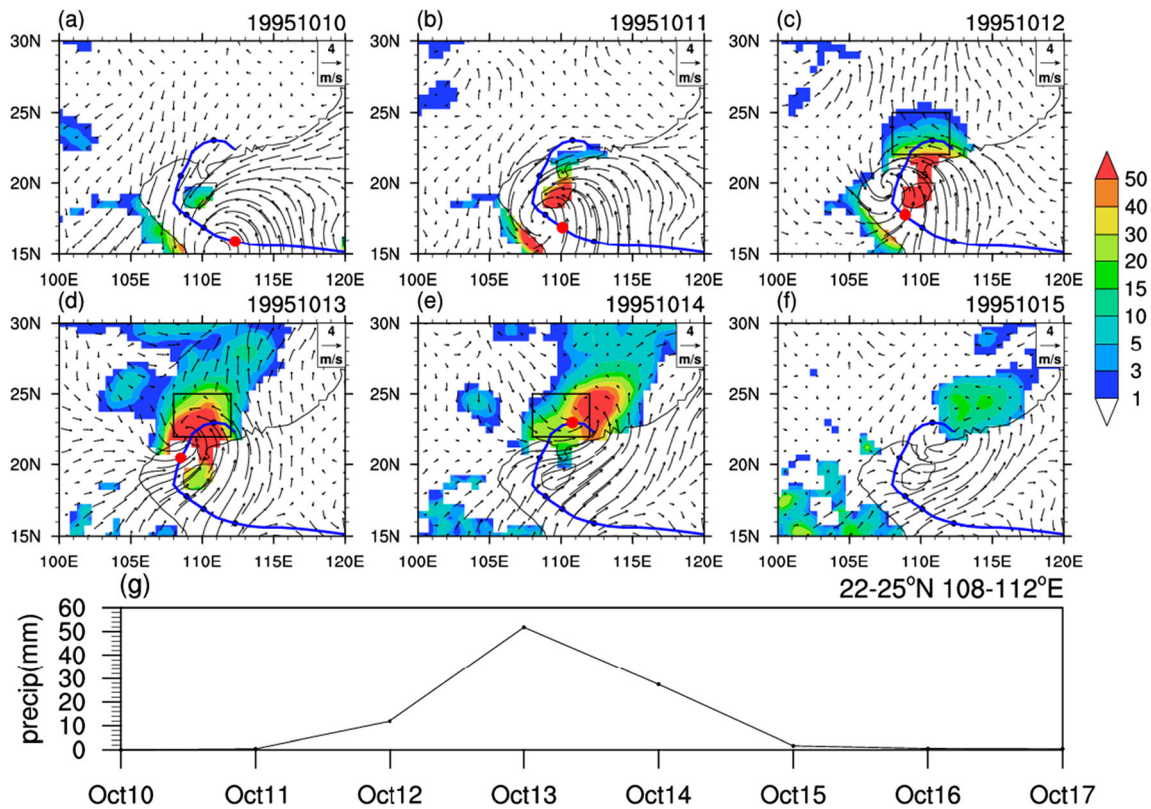


Fig. 1 (a-f) Precipitation amount (shading) (unit: mm) and wind anomalies (vector) (unit: m/s) at 10 m during October 10–15, 1995. (g) Precipitation amount averaged over the area of 22–25° N and 108–112°

E. The red dots represent the location of the cyclone. Blue line represents the best track of the cyclone

2.2.3 Linear trends of precipitation and contributions of three factors

We use multiple linear regression to analyze the contribution of intensity, duration, and frequency to the amount of precipitation. Taking the 1-to-3-day events as an example, the amount of precipitation of the 1-to-3-day PE can be written as follows:

$$P_{j,1-3day} = \beta_0 + \beta_1 \bar{I}_{j,1-3day} + \beta_2 \bar{D}_{j,1-3day} + \beta_3 N_{j,1-3day} + \epsilon_j \tag{7}$$

where beta are regression coefficients to be determined and epsilon is the residual of linear regression that is related to the nonlinear effect. The intensity, duration, and frequency are calculated using the linear regression:

$$\bar{I}_{j,1-3day} = \alpha_1 j + \alpha_0 + \epsilon_{\bar{I},j} \tag{8}$$

$$\bar{D}_{j,1-3day} = \gamma_1 j + \gamma_0 + \epsilon_{\bar{D},j} \tag{9}$$

$$N_{j,1-3day} = \kappa_1 j + \kappa_0 + \epsilon_{N,j} \tag{10}$$

where, $\alpha_1, \kappa_1, \gamma_1$ is the trend of the intensity, duration, and number of 1-to-3-day events, respectively; $\alpha_0, \kappa_0, \gamma_0$ denotes the intercept; $\epsilon_{\bar{I},j}, \epsilon_{\bar{D},j}, \epsilon_{N,j}$ is the residual of linear regression that is related to the nonlinear effect. Linear trends are calculated using the least square fitting method and the significance of the linear trends is estimated using Student’s *t* test. Accordingly, the change of rainfall amount of the 1-to-3-day PE is as follows:

$$\begin{aligned} \frac{dp_{j,1-3day}}{dj} &= \beta_1 \alpha_1 + \beta_2 \gamma_1 + \beta_3 \kappa_1 + \beta_1 \frac{d\epsilon_{\bar{I},j}}{dj} \\ &+ \beta_2 \frac{d\epsilon_{\bar{D},j}}{dj} + \beta_3 \frac{d\epsilon_{N,j}}{dj} + \frac{d\epsilon_j}{dj} \end{aligned} \tag{11}$$

Write the amount of precipitation using the linear regression:

$$P_{j,1-3day} = A_j + B + E_j \tag{12}$$

where *A* is the overall trend of 1-to-3-day PE (mm/year), *B* is the intercept, and *E* is the residual of linear regression that is related to nonlinear effect. Then, we have the following:

$$\frac{dp_{j,1-3day}}{dj} = A + \frac{dE}{dj} \tag{13}$$

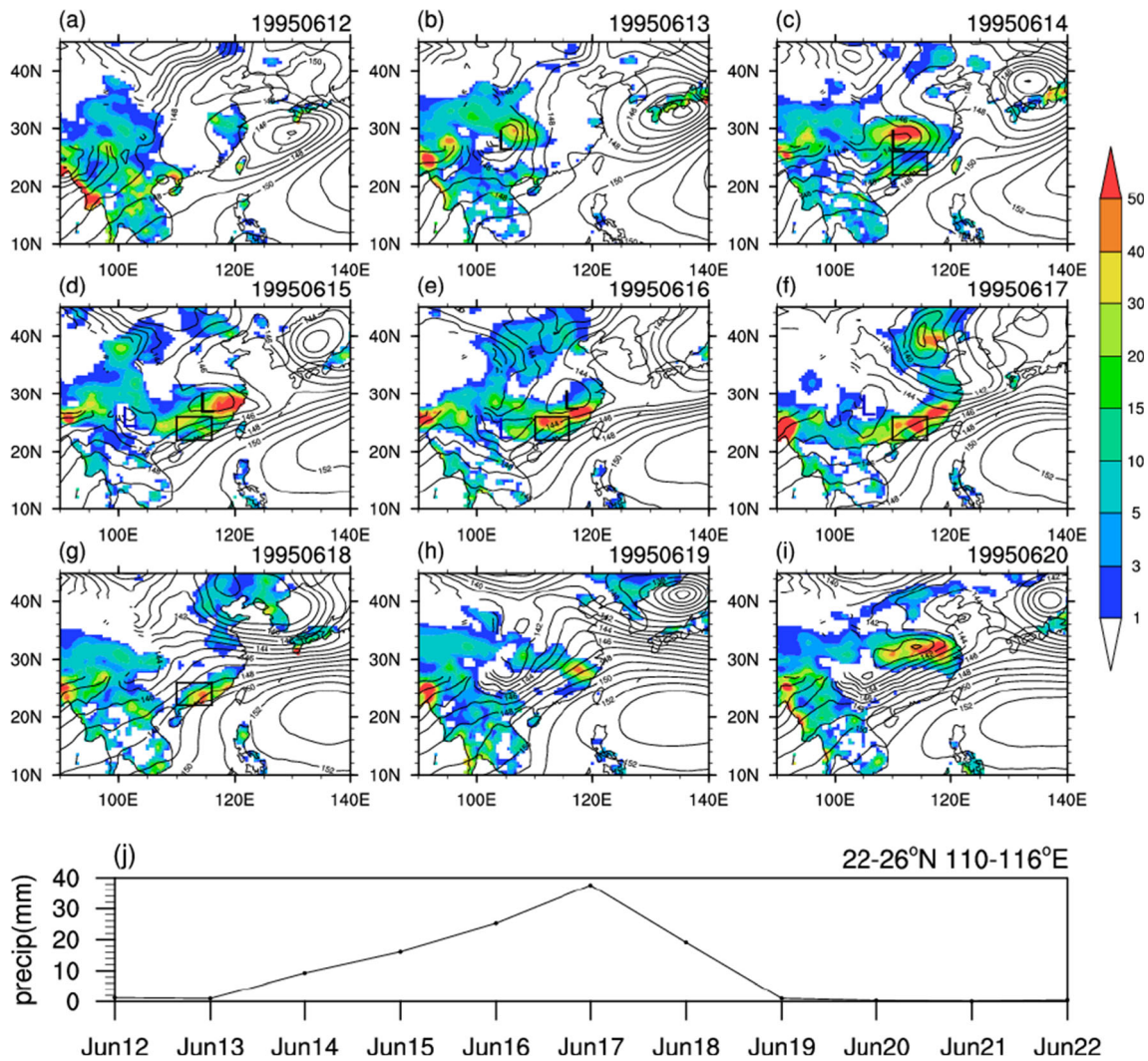


Fig. 2 (a–i) Precipitation amount (shading) (unit: mm) and geopotential height (contours) (unit: gpm) at 850 hPa during June 12–20, 1995. (j) Precipitation amount averaged over the area of 22–26° N and 110–116° E. L denotes the low system

Comparing Eqs. (11) and (13), we get the following:

$$A = \beta_1 \alpha_1 + \beta_2 \gamma_1 + \beta_3 \kappa_1 + \beta_1 \frac{d\epsilon}{dj} + \beta_2 \frac{d\bar{D}_j}{dj} + \beta_3 \frac{d\epsilon_{N,j}}{dj} + \frac{d\epsilon_j}{dj} - \frac{dE}{dj} \quad (14)$$

The first, second, and third terms represent contribution related to the intensity, frequency, and duration, respectively. The sum of rest terms is the nonlinear contribution.

2.2.4 Interdecadal changes in precipitation and contributions of three factors

In this article, interdecadal change of precipitation amount is determined by three factors, taking, for example, the 1-to-3-day events,

$$\begin{aligned} \Delta P_{1-3\text{day}} = & N_{1-3\text{day}} \bar{D}_{1-3\text{day}} \Delta I_{1-3\text{day}} \\ & + N_{1-3\text{day}} \bar{I}_{1-3\text{day}} \Delta D_{1-3\text{day}} \\ & + \bar{I}_{1-3\text{day}} \bar{D}_{1-3\text{day}} \Delta N_{1-3\text{day}} + O(\rho) \end{aligned} \quad (15)$$

where $N_{1-3\text{day}}$ and $\bar{D}_{1-3\text{day}}$ are the average number and the average duration of 1-to-3-day PEs. $\Delta I_{1-3\text{day}}$ is the changes in the intensity of 1-to-3-day PEs. The first, second, and third terms are the contributions of intensity, duration, and frequency to the interdecadal change of precipitation of 1-to-3-day PEs.

2.2.5 Life spans of circulation variations related to precipitation events

In general, the PEs with different durations are linked to circulation systems with different life spans. In this study, we

attributed the 1-to-3-day PEs to the wind variations with life span shorter than 9 days, the 4-to-7-day PEs to wind variations with a life span of 9–19 days, the 8-to-14-day PEs to wind variations with a life span of 19-to-29-days, and the over-14-day PEs to wind variations with a life span of more than 29 days. The above PE duration-wind life span relationship is based on the assumption that precipitation falls in about half of the life span of wind variations. For example, for an intraseasonal variations of 20 days, it is likely that the precipitation occurs in the wet phase of the intraseasonal variations that is about 10 days. In the present study, we analyze the wind variations corresponding to a specific type of PEs based on the above relationship.

2.3 Climatological features of the precipitation events

In this section, we analyze the climatological features of summer precipitation of the four types of PEs and their contributions to the total summer precipitation. This provides a background of the changes in the precipitation amount of the four types of PEs in the next two sections.

The highest summer mean rainfall amount is observed in tropical regions with obvious coastal or orographic features: the west coasts of the Indian subcontinent, the south hills of the Himalaya, and the east and west coasts of the Indo-China Peninsula (Fig. 3a). The total precipitation amount is high in the southeast and generally decreases towards central Asia. This pattern is resulted from the transportation of water vapor by the Asian summer monsoon. Water vapor becomes less over inland areas than the coastal area because it gets further away from the major water vapor source regions (Wu et al. 2019b). The total precipitation amount is moderate over the mid-latitude regions, which is related to the activity of eastward-moving circulation systems along the mid-latitudes. The precipitation amount of the 1-to-3-day events over the middle latitudes north of 30°N is higher than the other events (Fig. 3b–e). The precipitation amount of the 4-to-7-day events displays two regions with higher values: one located at middle latitudes to the north of 45°N and the other located to the south of 35°N (Fig. 3c). The precipitation amount of the 8-to-14-day events displays similar features but with lower values than the 4-to-7-day events over the middle latitudes (Fig. 3d). The precipitation amount of the over-14-day events is much higher in the lower latitude regions than in the higher latitude regions (Fig. 3e).

The spatial pattern of the fractional contributions of the four types of PEs to the total precipitation amount shows distinct features. The contribution of the 1-to-3-day PEs to climatological mean precipitation over central Asia is much larger than the other events (Fig. 4a–d). This is due to the dominant impact of short-duration synoptic weather systems along the middle latitudes over this region (Liu and Wu 2016). Longer duration events, the 8-to-14-day and over-14-day

PEs, contribute more to the summer precipitation amount over the tropical regions than the shorter duration events. Over-14-day PEs have a dominant contribution to the precipitation amount along the west coasts of the Indian subcontinent and Indo-China Peninsula and the south hills of the Himalaya (Fig. 4d). This is distinct from the other events whose contribution to the precipitation amount is relatively small along the west coasts. The above results are consistent with Liu and Wu (2016) whose analysis was based on a shorter time period of 1951–2006.

The distinct distribution of fractional contributions among the four types of PEs indicates that the PEs with different durations are linked to circulation systems with different characteristics. The over-14-day PEs are likely related to slow-moving convective systems from the equatorial region, such as the 30-to-60-day intraseasonal oscillations (ISOs). Previous studies have shown that the 30-to-60-day ISOs tend to move eastward in the tropics, which are accompanied by northward extension of the rain bands (e.g., Annamalai and Slingo 2001; Kemball-Cook and Wang 2001). When these precipitation bands hit the west coasts, the topographic effects lead to a large precipitation amount there. In contrast, synoptic systems, such as tropical storms, and shorter period ISOs, such as the quasi-biweekly ISOs, tend to move westward in the tropical Indo-western Pacific regions (e.g., Mao and Chan 2005; Kikuchi and Wang 2009). The precipitation induced by these circulation systems is mostly in the eastern part of the tropical land regions. Over the middle latitude regions, short-duration synoptic systems are dominant. As a result, the short-duration PEs have more contribution to the precipitation amount in the middle latitudes.

2.4 Linear trends

The trend of summer precipitation has been a topic of previous studies (e.g., Liu et al. 2005; Zhai et al. 2005; Ding et al. 2007; Lu et al. 2014). In this section, we analyze the contribution of the four types of PEs to the long-term trend of summer precipitation in China during 1951–2015. We are concerned with which type of PEs has a relatively large contribution to the long-term trend of summer precipitation in the concerned regions. In addition, we explore which characteristics of PEs (frequency, duration, and intensity) have the largest effect on the precipitation trends in each PE.

Summer precipitation shows a decreasing trend over North China and an increasing trend in northwestern and southern China (Fig. 5a). This is consistent with previous studies (Liu et al. 2005; Zhai et al. 2005; Ding et al. 2007; Lu et al. 2014). The increasing trends are also seen in Korea and most of the Indo-China Peninsula. There are decreasing trends in central India and Burma. In the following, we focus on the trends in several regions of China where the trends are significant at the 90% confidence level.

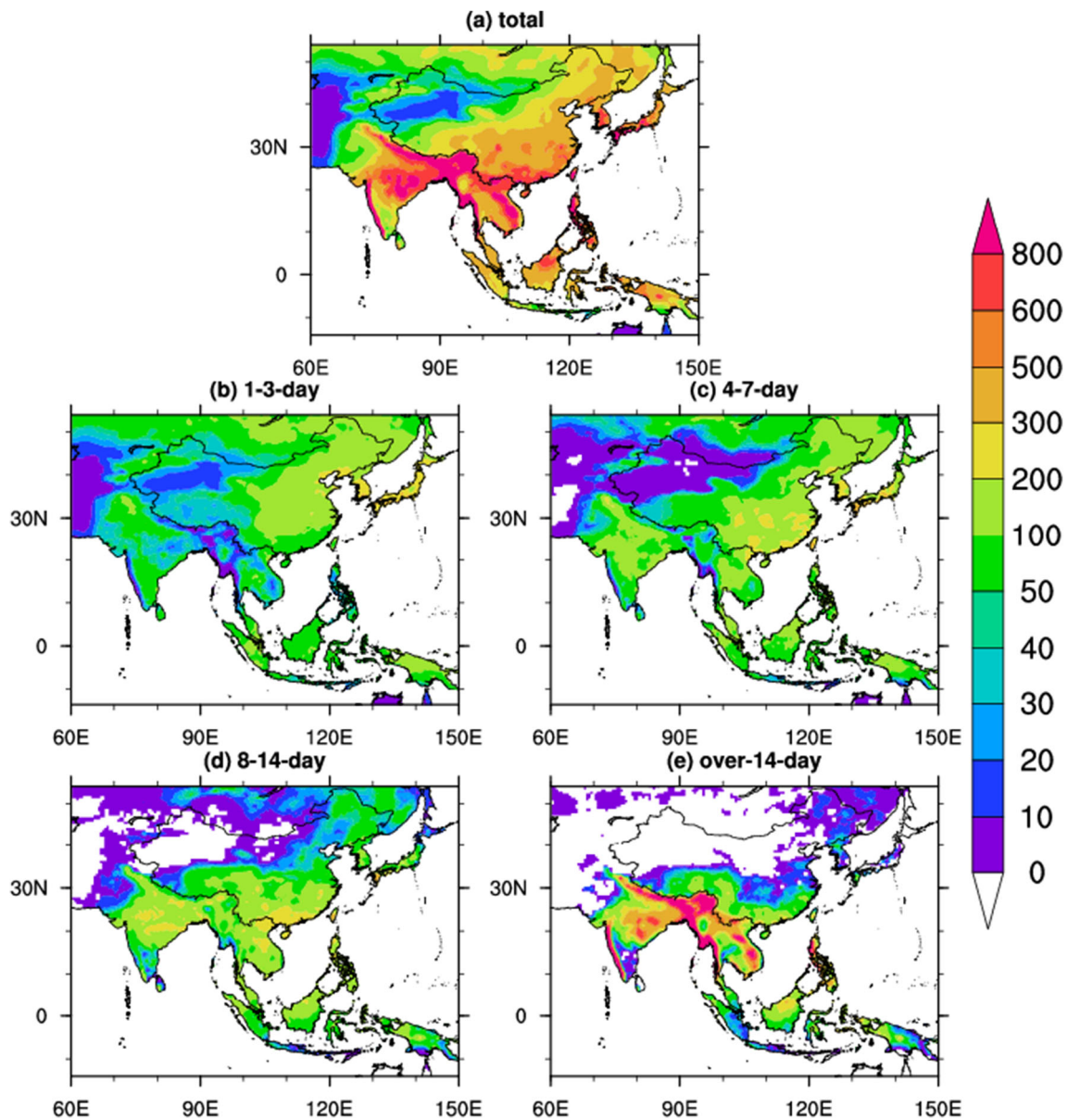


Fig. 3 Climatological mean summer precipitation (mm) for the period 1951–2015. (a) Total amount and the amount due to the precipitation events with durations of (b) 1–3 days, (c) 4–7 days, (d) 8–14 days, and (e) over 14 days

The decreasing trend of precipitation in North China and the increasing trend of precipitation in northwestern China are mainly related to the shorter duration events, the 4-to-7-day and 1-to-3-day events (Fig. 5a–c). The 8-to-14-day and 4-to-7-day events contribute to the increasing trend of precipitation over southern China (Fig. 5a, c, d). The trends of precipitation over tropical regions are mainly attributed to over-14-day events (Fig. 5a, e). For a quantitative estimation, we calculate area-mean trends of precipitation in the above regions. The precipitation amount in North China has a linear trend of -0.75 mm/year or 2.7% /decade (the climatological mean amount is 274.8 mm) (Fig. 6a). The 4-to-7-day events account for 48.6% of the linear trend over North China. In the northwestern China, the precipitation amount increases at 0.25 mm/

year or 4.5% /decade (the climatological mean amount is 55.6 mm) (Fig. 6f). The 4-to-7-day events account for 41.6% of the trend of the total amount over northwestern China. The linear trend over southern China is 1.29 mm/year or 2.6% /decade (the climatological mean is 490.2 mm) (Fig. 6k). The 8-to-14-day events have a contribution rate of 46.4% to the trend in the total amount and the 4-to-7-day events contribute another 38.6% to the trend of precipitation over southern China.

Changes in precipitation can be caused by frequency, intensity, and duration changes. We calculate the fractional contributions of intensity, duration, and frequency trends to the trends of the total amount using Eqs. (7–10, 12, 14) in Section 2. Results are shown in Fig. 6b–e, g–j, and l–o,

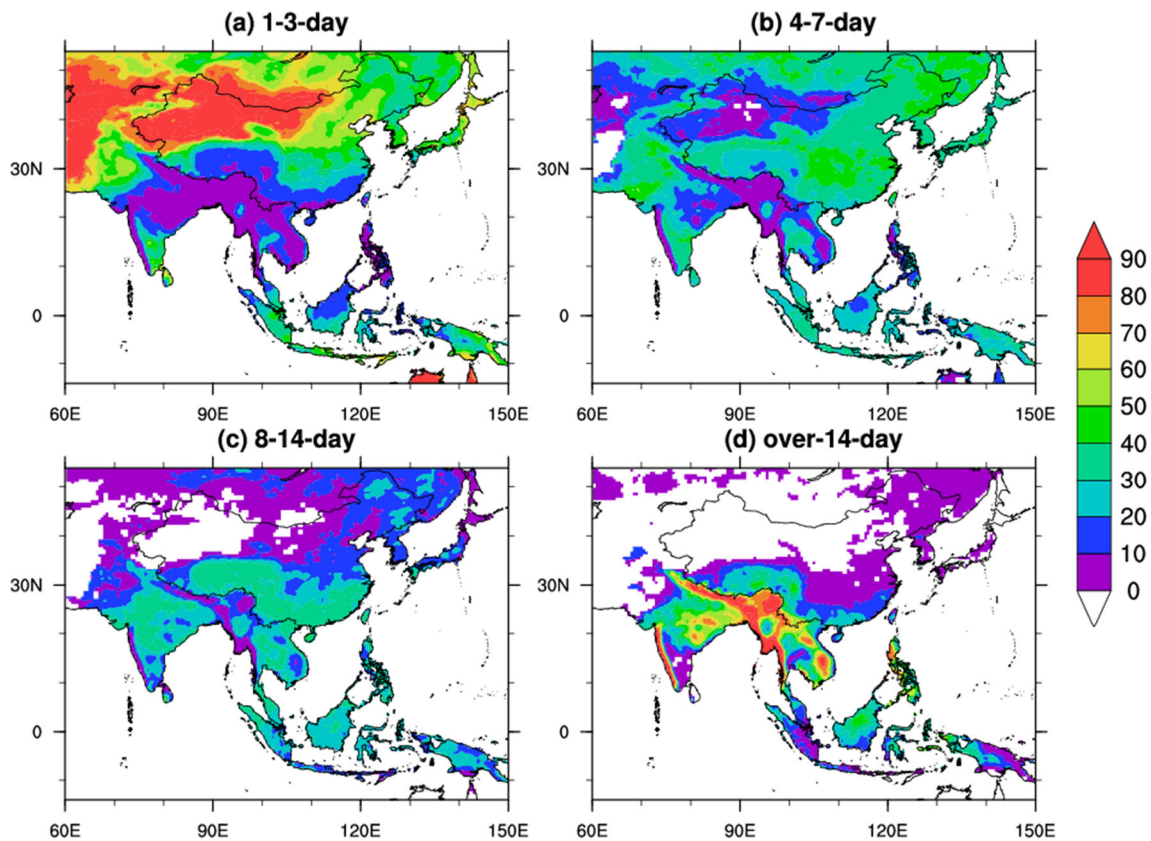


Fig. 4 Fractional contribution (unit: %) of the precipitation events with durations of (a) 1–3 days, (b) 4–7 days, (c) 8–14 days, and (d) over

14 days to climatological mean total summer precipitation amount for the period 1951–2015

respectively, for the above three regions. The contribution of the 4-to-7-day events to the decreasing trend of precipitation in North China is mainly due to the decrease of the number of events (Fig. 6c). The contribution of the 1-to-3-day events to the decreasing trend is related to both intensity and number (Fig. 6b). The contribution of the 8-to-14-day events is mainly due to the intensity (Fig. 6d). The contribution of PEs to the increasing trend of precipitation in northwestern China is all related to the number change (Fig. 6g–j). In addition, the intensity change of the 4-to-7-day events has a positive contribution to the increasing trend of precipitation. The positive contribution of 4-to-7-day and 8-to-14-day PEs to the increasing trend in southern China is attributed to both the number and intensity changes. The positive contribution of the 1-to-3-day PE is mainly due to the intensity change.

2.5 Interdecadal changes

The interdecadal variability of summer precipitation in China has been studied by previous studies. Four interdecadal changes have been recognized since the 1950s, which occurred around the mid-1960s in North China, late 1970s in Northeast China and the Yangtze River region, and early 1990s in southern China and late 1990s in northern China (e.g., Yan et al. 1990; Gong and Wang 2000; Ding et al.

2008; Liu et al. 2011). Our inspection of area-mean summer precipitation evolution confirms the above four interdecadal changes in summer precipitation (not shown). In this section, we document the contribution of the four types of PEs to the above four interdecadal changes of summer precipitation in China and the effects of frequency, duration, and intensity changes for precipitation changes in each PE.

The precipitation decrease over North China during the mid-1960s has a larger contribution from the 4-to-7-day and 8-to-14-day events (Fig. 7a–f). The contribution of 1-to-3-day and over-14-day events is small. The decrease of precipitation of the 4-to-7-day events is largely due to the decrease in the number of events (Fig. 7h). The decrease of precipitation of the 8-to-14-day events is due to the nonlinear effect (Fig. 7i). The above precipitation decrease is associated with the lower-level northerly wind change extending from Northeast China to southern China (Fig. 7a–d) that reduces the northward transport of moisture from the lower latitudes.

To understand the impact of the circulation pattern on the precipitation change, we construct wind anomaly distribution corresponding to the 4-to-7-day PEs. The composite wind anomalies are obtained based on averaging 9-to-19-day filtered daily 850 hPa wind anomalies over the days when precipitation reaches 1 mm in half of the grids in the domain of 34–43° N and 108–118° E that is defined as a 4-to-7-day

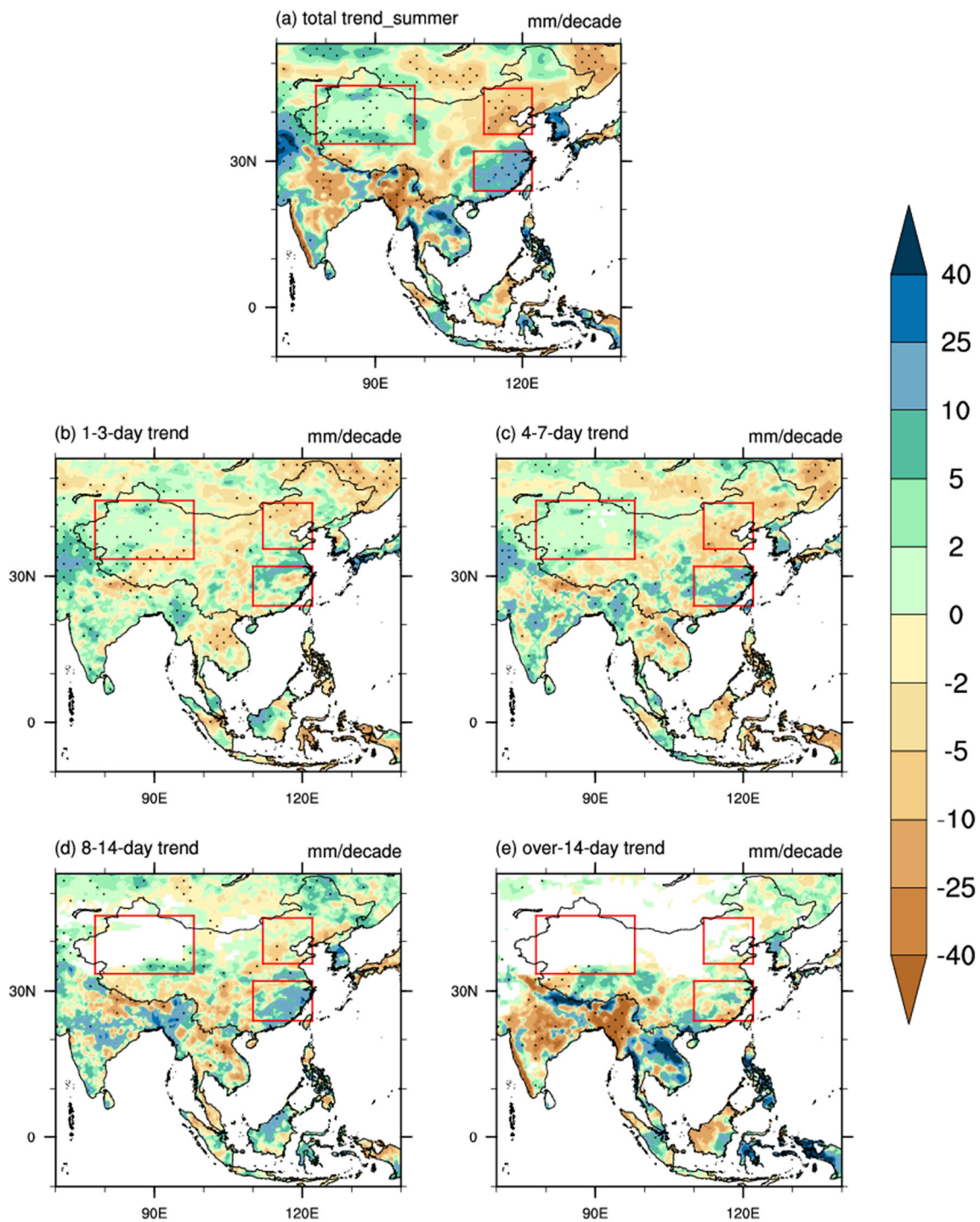


Fig. 5 Spatial distribution of trends (mm/decade) of summer precipitation over the period 1951–2015. (a) Total precipitation and (b–e) the precipitation due to precipitation events with durations of (b) 1–3 days, (c) 4–7 days, (d) 8–14 days, and (e) over 14 days. Dots denote trends significant

at the 90% confidence level. The three boxes denote the domain of north-west China, North China, and southern China used in calculation of area mean in Fig. 6

event. Although this definition is subjective, the wind anomaly pattern leading to precipitation events can be captured using such a definition as shown below (e.g., Fig. 8a). This indicates that the definition is suitable and reasonable. As the wind system leading to precipitation in a region usually moves

with the time, use of a slightly more or less strict criterion may obtain larger or weaker composite wind anomalies with less or more days satisfying the criterion. However, the general features are expected to remain similar. The 9-to-19-day time band is chosen for temporal filtering because a 4-to-7-day

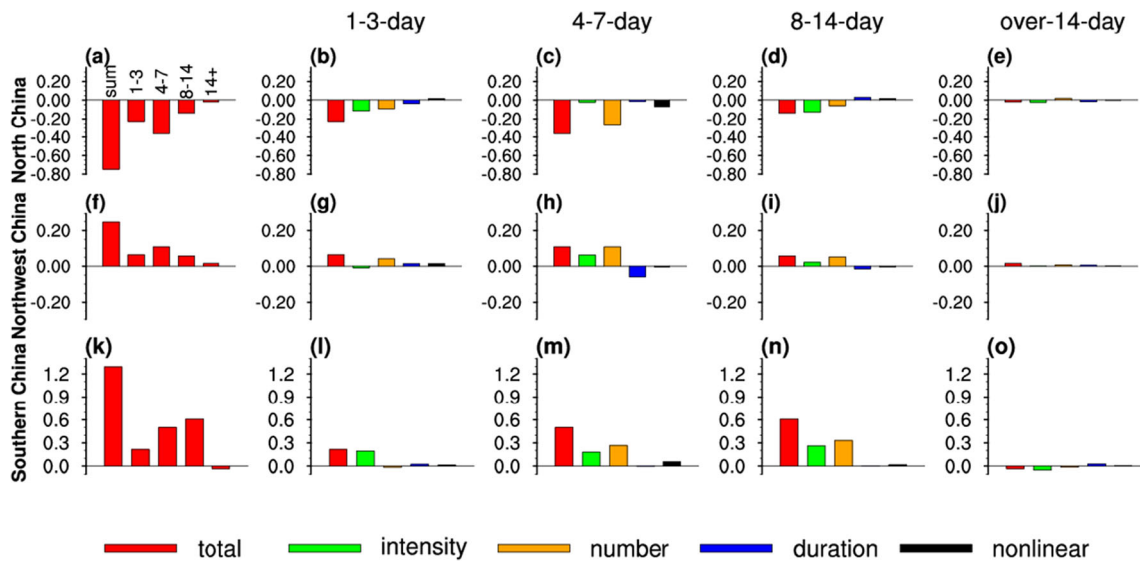


Fig. 6 (a) Trends of total summer precipitation and contributions of the precipitation events with durations of 1–3 days, 4–7 days, 8–14 days, and over 14 days over North China. (b–e) Trends of precipitation (red) due to the precipitation events with durations of (b) 1–3 days, (c) 4–7 days, (d) 8–14 days, and (e) over 14 days over North China and the contributions due to changes in intensity (green), frequency (yellow), duration (blue) and the residual part associated with the nonlinearity (black). (f–j) and (k–o) are similar to (a–e) except over northwest China and southern China (k). The unit is mm/year

event is likely corresponding to a half period of 9-to-19-day wind variations. An apparent lower-level cyclone is observed over North China, accompanied by an anticyclone on its east side in the composite wind anomaly field over the period of 1951–2015 (Fig. 8a). We then project 9-to-19-day filtered

daily 850 hPa wind anomalies on the above wind composite field in the domain of 29–48° N and 98–128° E. The probability density function (PDF) of projection coefficient is constructed for 1965–1974 and 1955–1964, respectively (Fig. 8b). Apparently, the PDF of the projection coefficient is

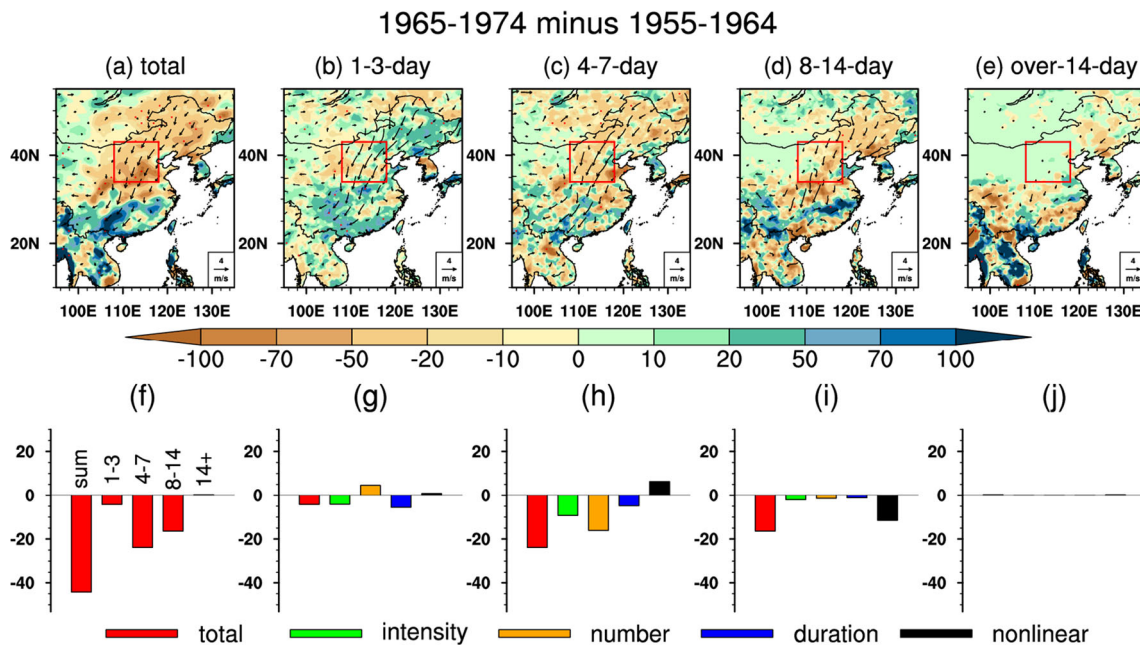


Fig. 7 Spatial distribution of interdecadal change of summer precipitation (shading) and 850 hPa winds (vector, scale at the right-bottom corner) at the mid-1960s. (a) Total precipitation and (b–e) precipitation of events with durations of (b) 1–3 days, (c) 4–7 days, (d) 8–14 days, and (e) over 14 days. (f) Interdecadal change of total summer precipitation at the mid-1960s and contributions of the precipitation events with durations of 1–3 days, 4–7 days, 8–14 days, and over 14 days over North China. (g–j) Trends of precipitation (red) due to the precipitation events with durations of 1–3 days, 4–7 days, 8–14 days, and over 14 days over North China and the contributions due to changes in intensity (green), frequency (yellow), duration (blue) and the residual part associated with the nonlinearity (black). Dots denote precipitation changes significant at the 90% confidence level. The box in Figs. a–e denotes the domain used in calculation of area mean in Figs. f–j. Unit: mm

different in 1965–1974 and 1955–1964 with the difference of the Kolmogorov-Smirnov statistic (Fig. 8c) reaching the 99% confidence level. It implies that the activity of the cyclonic wind anomaly pattern over North China leading to precipitation of the 4-to-7-day events was reduced after the mid-1960s. During 1965–1974, the PDF is skewed towards negative values, which corresponds well with the decrease in precipitation of 4-to-7-day events over North China. Conversely, during 1955–1964, active spells occurred more frequently as there was more cyclonic activity.

Summer precipitation along the Yangtze River Valley experienced a notable regime shift at the late 1970s (Fig. 9a) (Ding et al. 2008; Liu et al. 2011; Liu and Wu 2016). A concurrent increase occurred in Northeast China (Fig. 9a). This spatial pattern is consistent with Liu and Wu (2016). Their analysis showed that the interdecadal changes around the late 1970s in total precipitation over the two regions are dependent on the changing number of precipitation days and the regrouping of events with different durations and intensities. However, they did not analyze which types of events contribute more. Here, we examine the fractional contributions of the four types of PEs to interdecadal change in the total amount of precipitation around the late 1970s. In both Northeast China and the middle Yangtze River valley, the 4-to-7-day and 8-to-14-day events contribute positively to the summer precipitation increase, the contribution of the over-14-day events is small, and the 1-to-3-day events have a negative contribution (Fig. 9a–f, k). The precipitation increase over Northeast China is associated with a lower-level cyclone and that over the middle Yangtze River valley is consistent with lower-level convergence in the wind change corresponding to the 4-to-7-day and 8-to-14-day precipitation events (Fig. 9c, d). In both Northeast China and the middle Yangtze River Valley, the increase of precipitation of the 4-to-7-day events is mainly due to the increase in the number

of events (Fig. 9h, m). The increase of precipitation of the 8-to-14-day events has a larger contribution from the nonlinear part (Fig. 9i, n). The negative contribution of the 1-to-3-day events is attributed to the decrease in the number of events (Fig. 9g, l). The above results indicate a tendency for the duration of PEs to become longer around the late 1970s.

The composite 9-to-19-day and 19-to-29-day filtered daily 850 hPa wind anomaly fields corresponding to the 4-to-7-day and 8-to-14-day PEs in the domain of 43–50° N and 121–128.5° E both features a cyclonic wind anomaly pattern over Northeast China (Fig. 10a, d). Similar to the analysis on the interdecadal changes around the mid-1960s, the PDFs are calculated based on the projection coefficient of filtered daily 850 hPa wind anomalies in the domain of 38–55° N and 111–138.5° E over two periods before and after the interdecadal change. Results indicate that the spatial pattern of the above wind anomalies has become more frequent over Northeast China since the late 1970s (Fig. 10b, e). The difference in PDFs exceeds the 99% confidence level according to the Kolmogorov-Smirnov statistic (Fig. 10c, f).

A similar analysis of the wind anomaly pattern and the PDFs has been conducted for the precipitation increase over the middle Yangtze River region. The composite 9-to-19-day and 19-to-29-day filtered daily 850 hPa wind anomaly distribution corresponding to the 4-to-7-day and 8-to-14-day events in the domain of 29–35° N and 104–112° E displays anomalous lower-level wind convergence in the above region (Fig. 11a, d). During the period before the change, the PDF of 9-to-19-day filtered daily 850 hPa wind anomalies in the domain of 24–40°N and 94–122° E tends to shift to negative values, which corresponds with the decrease of precipitation of the 4-to-7-day events (Fig. 11a–c). However, the difference of PDF of 19-to-29-day filtered wind anomalies before and after the change does not reach the 99% confidence level (Fig. 11e, f).

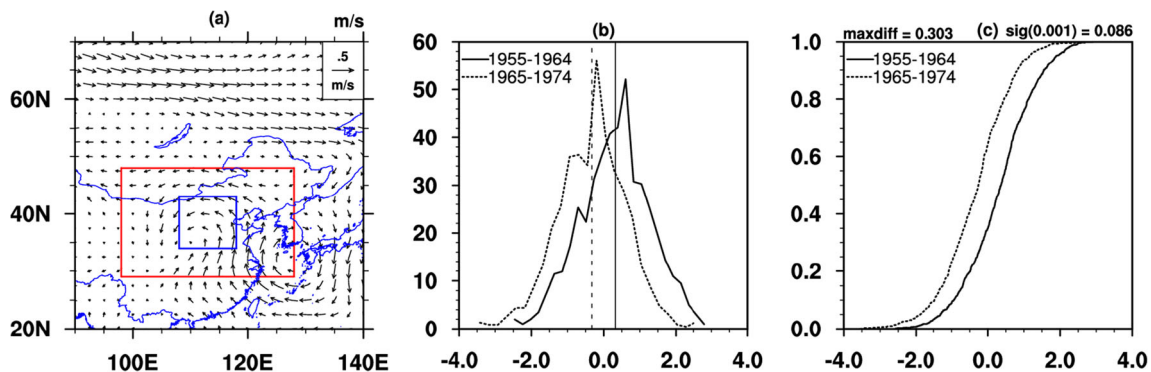


Fig. 8 (a) The composite 9–19-day filtered daily 850 hPa wind anomaly (m/s) distribution corresponding to the 4–7-day events in North China (denoted by the blue box). (b) The PDFs (unit: %) of projection coefficient of 9–19-day filtered 850 hPa daily wind anomalies based on the domain denoted by the red box for 1955–1964 (solid line) and 1965–

1974 (dash line), respectively. The vertical lines denote the mean project coefficients in the respective periods. (c) The Kolmogorov–Smirnov statistic of PDF for the period 1955–1964 (solid line) and 1965–

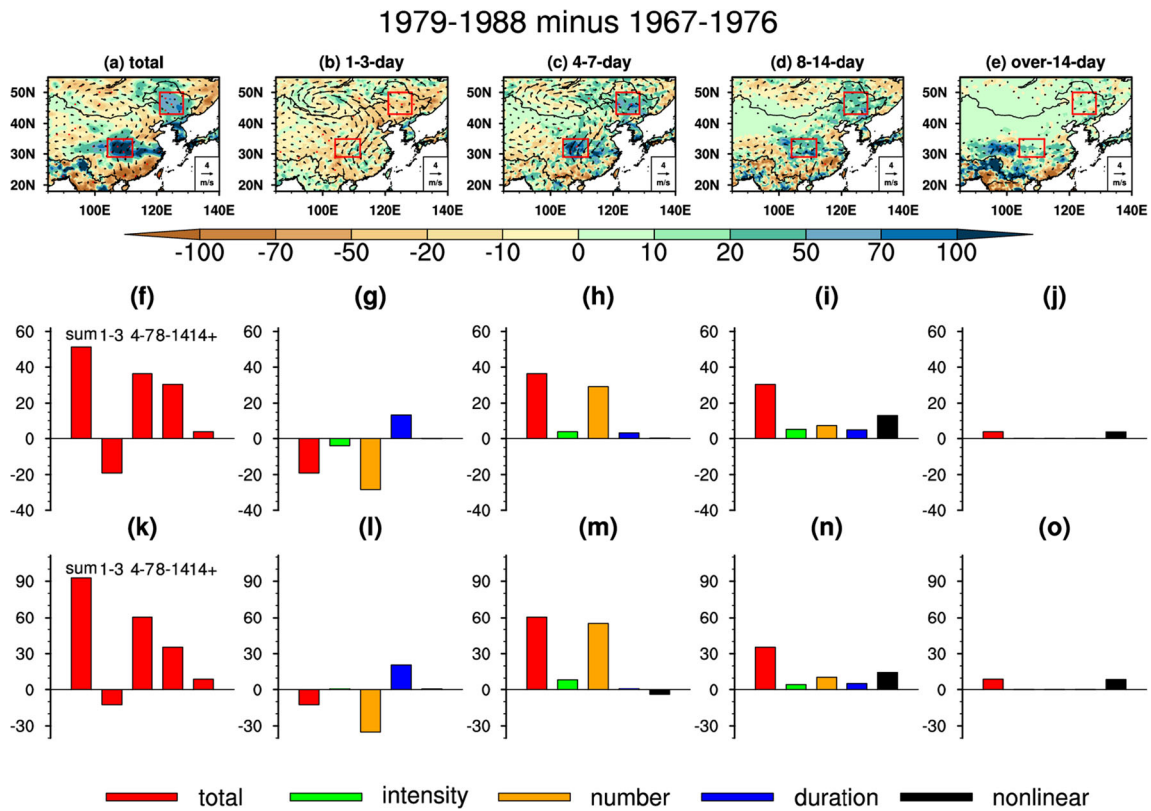


Fig. 9 As Fig. 7 but for the interdecadal change around the late 1970s in Northeast China and the middle Yangtze River. (f–j) are for Northeast China, (k–o) are the middle Yangtze River region

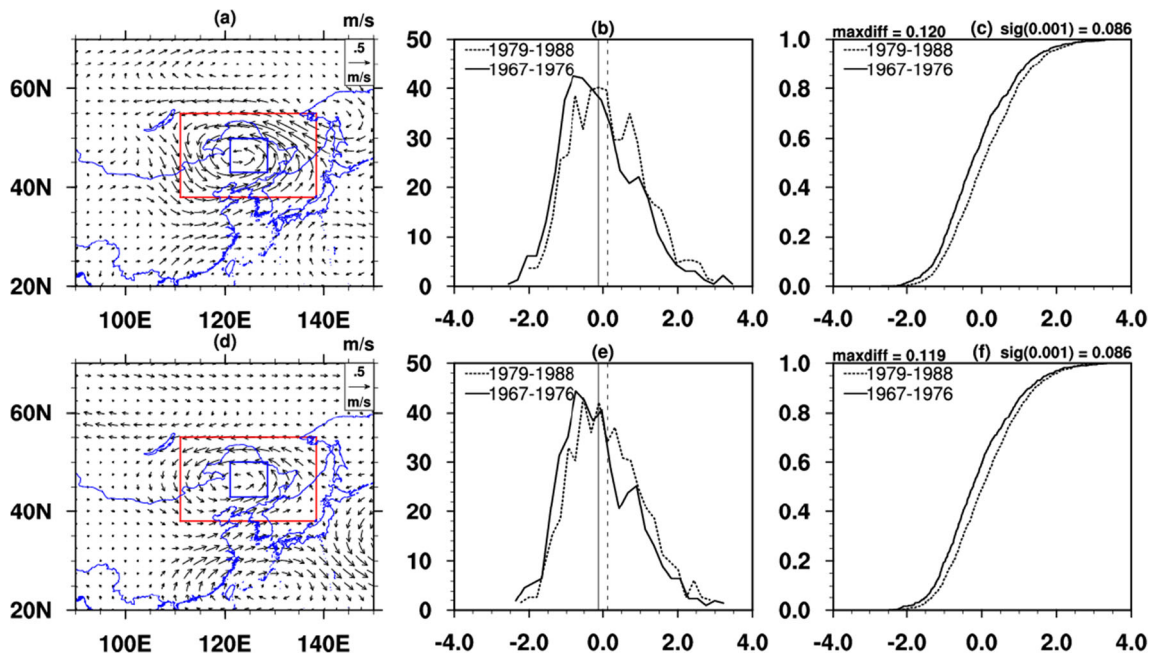


Fig. 10 The composite (a) 9-to-19-day and (d) 19-to-29-day filtered daily 850 hPa wind anomaly (m/s) distribution corresponding to the 4-to-7-day and 8-to-14-day events in Northeast China (denoted by the blue box). The PDFs (unit: %) of projection coefficient of (b) 9-to-19-day and (e) 19-to-29-day filtered daily 850 hPa wind anomalies based on the domain

denoted by the red box for 1967–1976 (solid line) and 1979–1988 (dash line), respectively. The vertical lines denote the mean project coefficients in the respective periods. The Kolmogorov–Smirnov statistic of PDFs of (c) 9-to-19-day and (f) 19-to-29-day filtered daily 850 hPa wind anomalies for 1967–1976 (solid line) and 1979–1988 (dash line)

A notable increase in summer rainfall over southern China occurred around 1992–1993 (Fig. 12a) (Ding et al. 2008; Wu et al. 2010). This shift has a larger contribution by longer duration events, especially the over-14-day events (Fig. 12a–f). This is consistent with Liu and Wu (2016) who showed that there is a significant decrease in the short duration events with weak intensities and a significant increase in the long duration events with strong intensities, especially the over-14-day events with mean intensities of 11–21 mm/day and over 23 mm/day. It was concluded that the interdecadal increase in the long duration (over-14-day) events may be attributed to the extended life cycles of persistent monsoon-related circulations since 1992. Our analysis shows that the precipitation increase of the over-14-day events is related to the non-linear effect (Fig. 12j). The precipitation increase of the 8-to-14-day events has an important contribution as well, with a larger part from the increase in the number of events (Fig. 12i). The main contribution of long-duration events to the above precipitation increase is consistent with the lower-level southerly wind change corresponding to the 8-to-14-day and over-14-day events (Fig. 12d, e).

To understand the precipitation change of the 8-to-14-day and over-14-day events over southern China, we construct composite 19-to-29-day and 29-to-61-day filtered daily 850 hPa wind anomalies corresponding to 8-to-14-day and over-14-day events in the domain of 22–28° N and 107–120° E. It is obvious that the precipitation increase is associated with anomalous cyclonic wind fields (Fig. 13a, d). In comparison, the spatial pattern of over-14-day events is more obvious than that of the 8-to-14-day events. The PDF of projected filtered daily 850 hPa wind anomaly fields in the domain of 17–33° N and 97–130° E in the period before the change shifts to negative values whereas that in the period

after the change shifts to positive values (Fig. 13b, e). The difference in PDFs exceeds the 99% confidence level according to the Kolmogorov-Smirnov statistic (Fig. 13c, f). In order to justify the reliability of PDF of circulation anomaly pattern derived from the NCEP-NCAR reanalysis 1, the calculation has been repeated using ERA-Interim data in the same sub-region for the same period. The obtained results validate those based on the NCEP-NCAR reanalysis.

The summer precipitation decrease around 1999 occurred over the mid-latitude regions, including northern China and Mongolia (Fig. 14a), as documented in previous studies (Wu et al. 2019a). The precipitation decrease has a larger contribution of the 4-to-7-day events (Fig. 14a–f), which is closely related to the reduced number of the 4-to-7-day events (Fig. 14f). The 8-to-14-day events have a supplementary contribution to the precipitation decrease in the above region (Fig. 14d, f). The above precipitation decrease is consistent with a lower-level anticyclone in the wind change (Figs. 14a–d).

The composite 19-to-29-day and 29-to-61-day filtered daily 850 hPa wind fields corresponding to the 4-to-7-day and 8-to-14-day events display an anomalous cyclone over the middle latitudes (Fig. 15a, d). A significant difference of PDF of projected filtered daily 850 hPa wind anomaly fields in the domain of 37.5–57.5° N and 90–140° E is seen for the 4-to-7-day events (Fig. 15b). The PDF tends to shift to negative values during 1999–2014, which is consistent with the reduced precipitation amount. The PDF difference between the two periods before and after 1999 exceeds the 99% confidence level according to the Kolmogorov-Smirnov statistic (Fig. 15c). The PDF of the projection coefficient based on the 8-to-14-day events displays similar features (Figs. 15e, f).

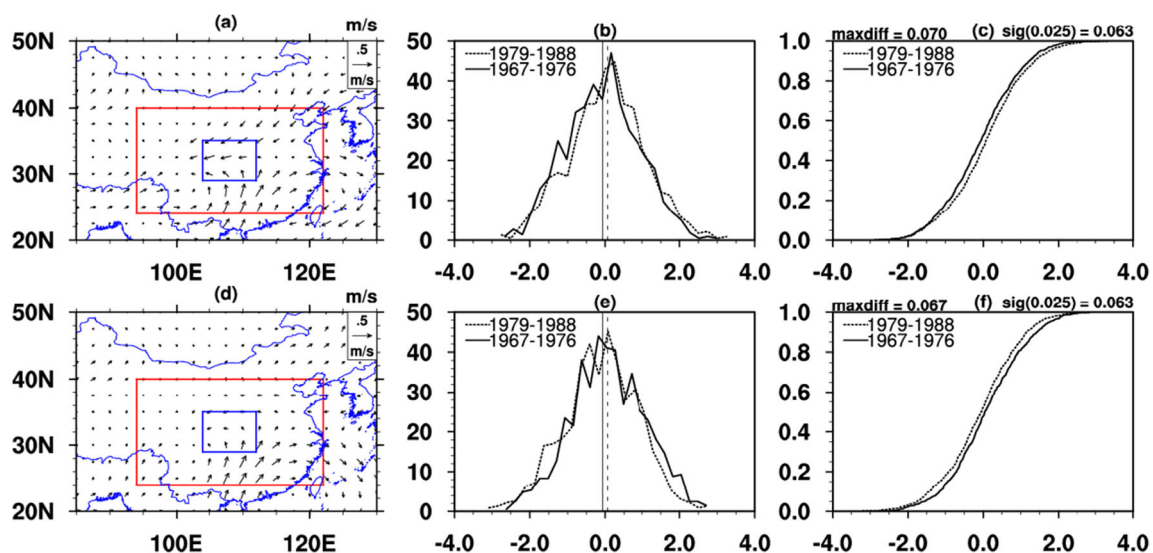


Fig. 11 As in Fig. 10 but for the middle Yangtze River region

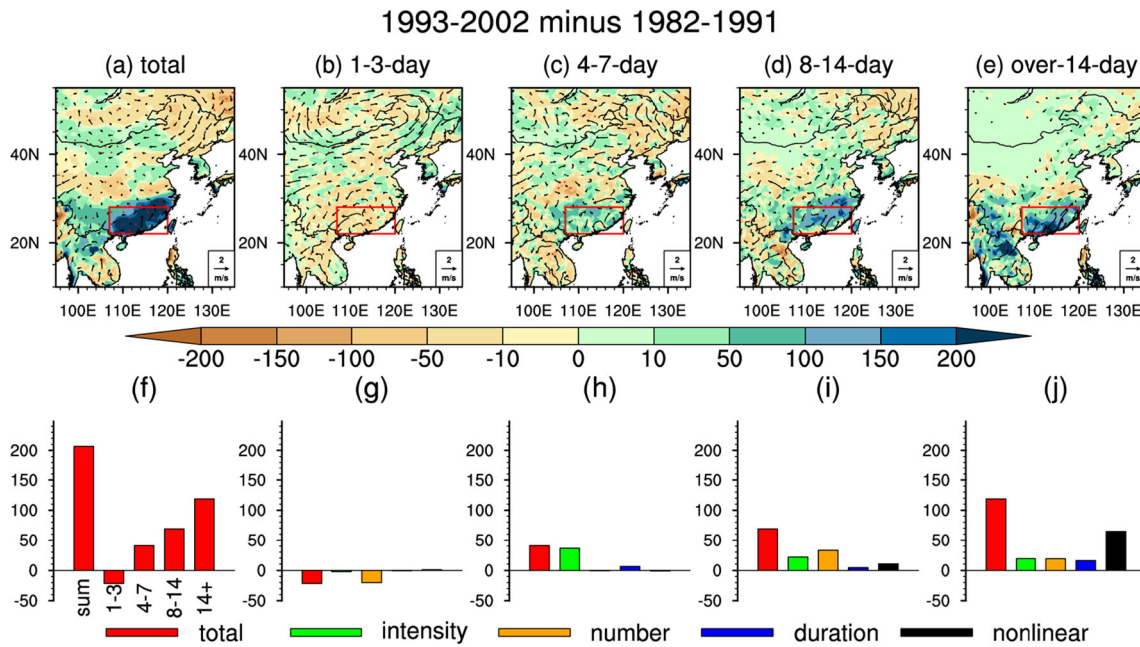


Fig. 12 As in Fig. 7 but for the interdecadal change around the early 1990s in southern China

3 Summary

On the basis of the APHRODITE daily precipitation data set, the present study investigates climatological features, regional trends, and interdecadal changes from the contributions of four types of precipitation events that are classified based on the duration of consecutive precipitation days. The circulation features corresponding to the interdecadal changes of precipitation are also analyzed in this study. The main findings of this study are summarized as follows.

The contribution of 1-to-3-day events to the climatology of summer precipitation over Central Asia is larger than the

contribution of the other events. Longer duration events, the 8-to-14-day and over-14-day events, contribute more to the summer precipitation amount over the tropical regions than the shorter duration events. Over-14-day precipitation events have the largest maximum contribution to the precipitation amount over the tropical areas, especially along the west coasts of the Indian subcontinent and Indo-China Peninsula.

The 4-to-7-day events have a dominant contribution to the trends in total precipitation amount over northwestern and North China during 1951–2015. The 8-to-14-day events play a more important part in the trends of summer precipitation in

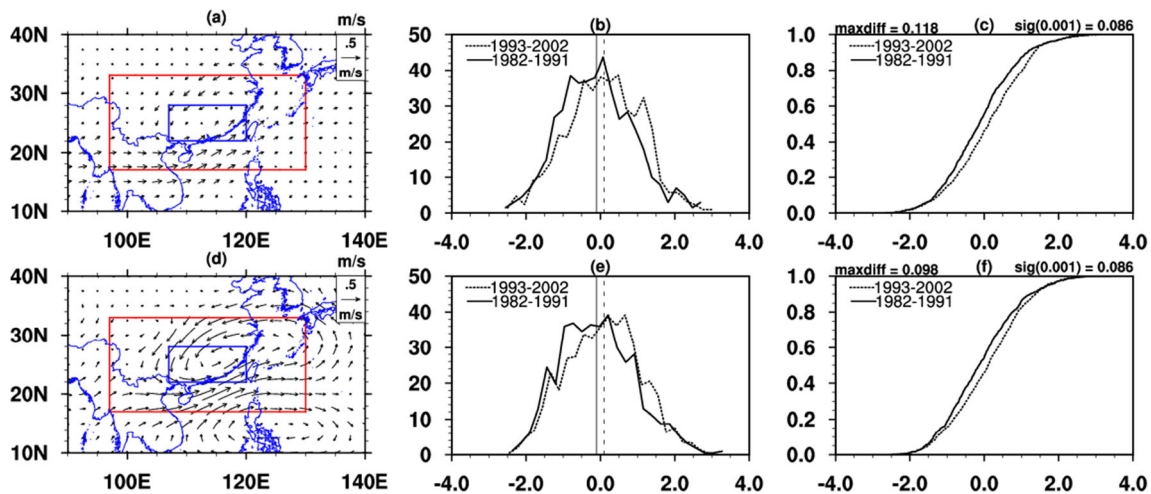


Fig. 13 The composite (a) 19-to-29-day and (d) 29-to-61-day filtered daily 850 hPa wind anomaly (m/s) distribution corresponding to 8-to-14-day and over-14-day events in southern China (denoted by the blue box). The PDFs of projection coefficient of (b) 19-to-29-day and (e) 29-to-61-day (e) filtered daily 850 hPa wind anomalies based on the domain

denoted by the red box for 1982–1991 (solid line) and 1993–2002 (dash line), respectively. The vertical lines denote the mean project coefficients in the respective periods. The Kolmogorov–Smirnov statistic of PDFs of (c) 19-to-29-day and (f) 29-to-61-day filtered daily 850 hPa wind anomalies for 1982–1991 (solid line) and 1993–2002 (dash line)

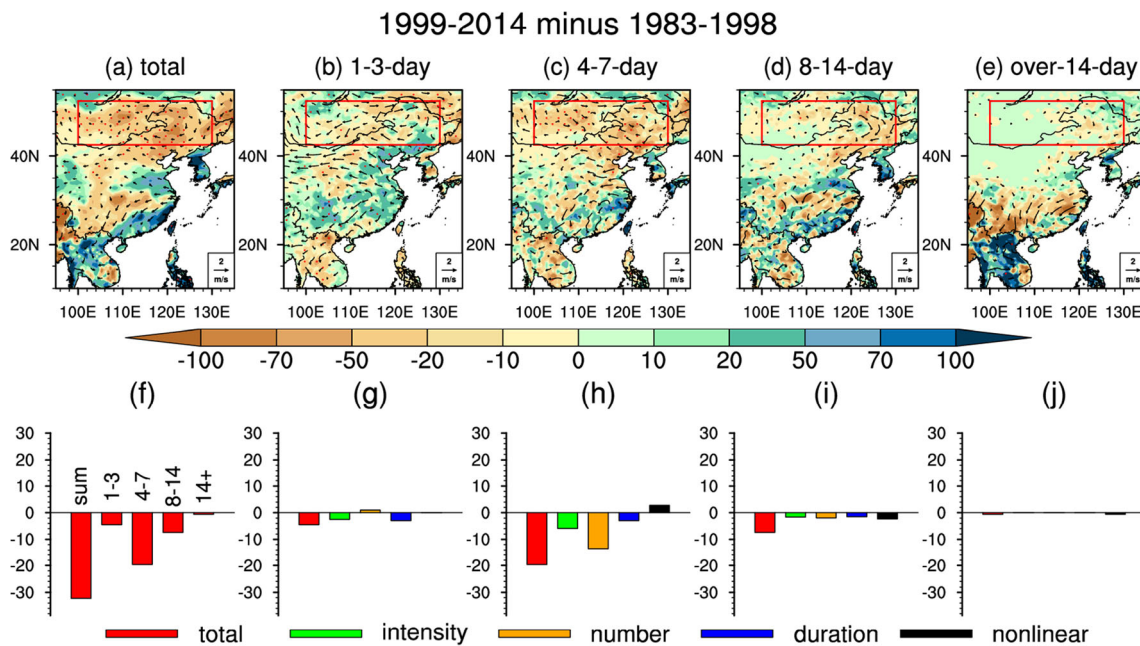


Fig. 14 As in Fig. 7 but for the interdecadal change around the late 1990s in the mid-latitude region

southern China during 1951–2015. In general, the frequency change of precipitation events has a greater contribution to the total precipitation changes than intensity and duration except for the over-14-day events in the three regions and the 1-to-3-day events over southern China.

The 4-to-7-day events contribute to the precipitation decrease in North China around the mid-1960s, the precipitation increase in Northeast China and the middle Yangtze River region around the late 1970s, and the precipitation decrease in the mid-latitude regions around the late 1990s. All these are mainly attributed to the change in the number of events. The 8-to-14-day events contribute to the late-1970s precipitation change in Northeast China and the middle Yangtze River region via the number of events. The precipitation increase

in southern China around 1993 is related to the over-14-day events.

The contributions of the three factors to the precipitation change of the four types of events are estimated by multiple linear regressions. One issue of concern is whether the estimated contributions of the three factors are affected by the correlations that may exist among the variations of the three factors. To address this issue, we have calculated the grid-point correlations of each pair of two factors. For the 4-to-7-day and 8-to-14-day events, the grid-point correlation is insignificant except for some isolated small regions. For the 1-to-3-day events, a significant intensity-duration correlation is observed, but not in North China, and a significant duration-number correlation is observed in eastern China. For the

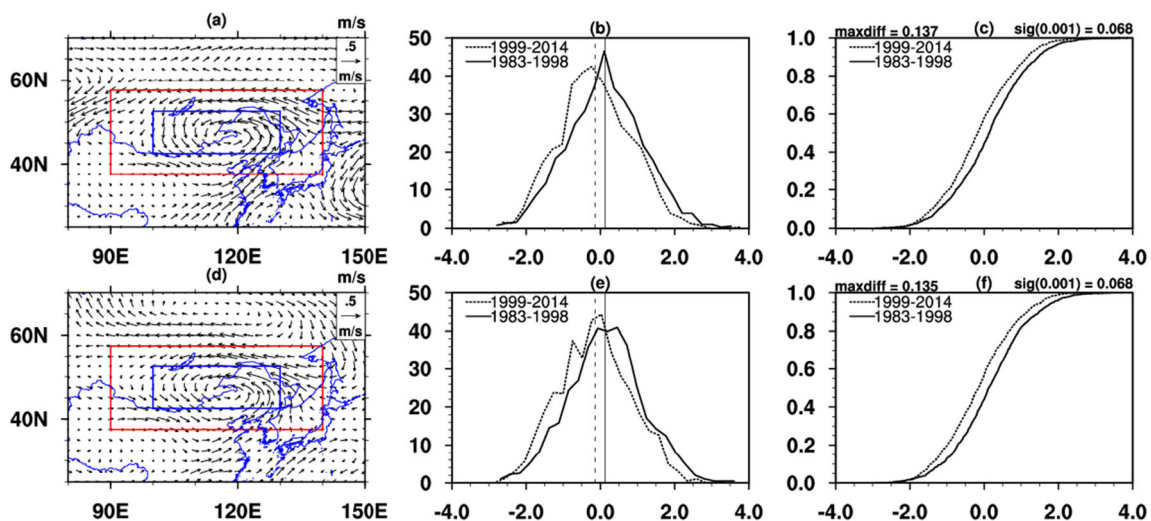


Fig. 15 As in Fig. 10 but for the interdecadal change around the late 1990s in the mid-latitude region

over-14-day events, a significant duration-number correlation is observed over India and Indo-China Peninsular. The above-mentioned significant correlation coefficient for the 1-to-3-day events is only 0.2–0.3. This indicates that the percentage of contributions related to the inter-dependence of two factors is not large and thus it does not affect much the contributions estimated based on the linear assumption. In addition, according to the present analysis, the precipitation changes in the concerned regions are mostly related to contributions of 4-to-7-day and 8-to-14-day events for which the three factors tend to be independent. For the over 14-day events, the correlation is insignificant in southern China. In addition, the residue term may include part of the contribution related to the interdependence of the three factors. Thus, we may say that the results obtained in the present study are not affected by the interdependence of the three factors. We note that the residual tends to display a normal distribution in the concerned regions of the present analysis.

A common feature of the four interdecadal precipitation changes is a decrease or an increase in the activity of cyclonic wind anomalies. This indicates an important role of higher frequency wind anomalies in the interdecadal changes of summer precipitation over China. The present results suggest that the interdecadal precipitation changes may be a result of changes in the activity of circulation systems with different life spans. This may provide useful information for understanding the reason for interdecadal changes in summer precipitation. While the present study reveals the impacts of wind variations with different life spans, it remains to be explored what are the source and propagation of these wind anomalies.

The present study focused on analyzing the four interdecadal changes in summer precipitation in China. There are other interdecadal changes in precipitation in China and in other regions. For example, an interdecadal increase in precipitation occurred in northwestern China around 1986 (Shi et al. 2003; Yin et al. 2009; Wang and Yan 2014). Our preliminary analysis indicates a major contribution of 1-to-3-day and 4-to-7-day precipitation events to the mid-1980s and the number of events is a dominant factor. Further analysis is needed to identify the changes in the relevant circulation pattern for these interdecadal changes. It is also worthy of investigation what are the relative contributions of the four types of precipitation events to interdecadal changes of precipitation in other regions and the associated changes in circulation patterns.

Previous studies assessed the contributions of changes in the number of days of precipitation with different intensities to long-term and interdecadal changes in summer precipitation over China (e.g., Liu et al. 2005; Zhai et al. 2005; Wen et al. 2015). The present study examined the changes in the intensity, duration, and frequency of the four types of precipitation events with different consecutive days and their respective contributions to long-term and interdecadal changes in

summer precipitation over China. This provides a new perspective of understanding the long-term and interdecadal changes of precipitation. Our results show that the precipitation events with long duration (4-to-7-day and 8-to-14-day) have a larger contribution to the observed long-term and interdecadal changes in summer precipitation over China. As these long-duration precipitation events are associated with circulation patterns with a life span of intraseasonal time scales, it implies that the long-term and interdecadal changes in summer precipitation are related to changes in the frequency of intraseasonal circulation patterns in the concerned region. This suggests that one should pay attention to changes in atmospheric intraseasonal oscillations when investigating the reasons for long-term and interdecadal precipitation changes.

Acknowledgments Comments of two anonymous reviewers are appreciated. The NCEP-DOE reanalysis data were obtained from <https://www.esrl.noaa.gov/psd/data/gridded/data.ncep.reanalysis.html>. The ERA-Interim data were obtained from <https://www.ecmwf.int/en/forecasts/datasets/reanalysis-datasets/era-interim>. The authors thank the Research Institute for Humanity and Nature (RIHN) for providing the Asian Precipitation Highly Resolved Observational Data Integration towards the Evaluation of Water Resources (APHRODITE) precipitation data set through its website (www.chikyu.ac.jp/precip/index.html).

Funding information This study is supported by the National Key Research and Development Program of China grant (2016YFA0600603) and the National Natural Science Foundation of China grants (41530425, 41775080, and 41721004).

References

- Annamalai H, Slingo JM (2001) Active/break cycles: diagnosis of the intraseasonal variability of the Asian summer monsoon. *Clim Dyn* 18:85–102. <https://doi.org/10.1007/s003820100161>
- Central Weather Bureau (CWB). 2004. <http://www.photino.cwb.gov.tw/tyweb/tyfnweb/htm/2004aere.htm>. Accessed 22 Apr 2006
- Dairaku K, Emori S, Oki T (2004) Rainfall amount, intensity, duration, and frequency relationships in the Mae Chaem watershed in south-east Asia. *J Hydrometeorol* 5:458–470. [https://doi.org/10.1175/1525-7541\(2004\)005<0458:RAIDAF>2.0.CO;2](https://doi.org/10.1175/1525-7541(2004)005<0458:RAIDAF>2.0.CO;2)
- Dee DP, Uppala SM, Simmons J, Berrisford P, Poli P, Kobayashi S, Andrae U, Balmaseda M, Balsamo G, Bauer P, Bechtold P, Beljaars CM, van de Berg L, Bidlot J, Bormann N, Delsol C, Dragani R, Fuentes M, Geer J, Haimberger L, Healy SB, Hersbach H, Hólm EV, Isaksen L, Kållberg P, Köhler M, Matricardi M, McNally P, Monge-Sanz BM, Morcrette JJ, Park BK, Peubey C, de Rosnay P, Tavolato C, Thépaut JN, Vitart F (2011) The ERA-Interim reanalysis: Configuration and performance of the data assimilation system. *Q J R Meteorol Soc* 137:553–597. <https://doi.org/10.1002/qj.828>
- Ding Y, Ren G, Zhao Z, Xu Y, Luo Y, Li Q, Zhang J (2007) Detection, causes and projection of climate change over China: an overview of recent progress. *Adv Atmos Sci* 24:954–971. <https://doi.org/10.1007/s00376-007-0954-4>
- Ding Y, Wang Z, Sun Y (2008) Inter-decadal variation of the summer precipitation in East China and its association with decreasing Asian

- summer monsoon. Part I: observed evidences. *Int J Climatol* 28: 1139–1161. <https://doi.org/10.1002/joc.1615>
- Francis JA, Vavrus SJ (2012) Evidence linking Arctic amplification to extreme weather in mid-latitudes. *Geophys Res Lett* 39:L06801. <https://doi.org/10.1029/2012gl0151000>
- Gong DY, Wang SW (2000) Severe summer rainfall in China associated with enhanced global warming. *Clim Res* 16:51–59. <https://doi.org/10.3354/cr016051>
- Guilbert J, Betts AK, Rizzo DM, Beckage B, Bombliès A (2015) Characterization of increased persistence and intensity of precipitation in the northeastern United States. *Geophys Res Lett* 42:1888–1893. <https://doi.org/10.1002/2015gl063124>
- Huang D, Zhu J, Kuang X (2011) Decadal variation of different durations of continuous Meiyu precipitation and the possible cause. *Chin Sci Bull* 56:424–431. <https://doi.org/10.1007/s11434-010-4241-x>
- Huang R, Liu Y, Feng T (2012) Interdecadal change of summer precipitation over Eastern China around the late-1990s and associated circulation anomalies, internal dynamical causes. *Chin Sci Bull* 58: 1339–1349. <https://doi.org/10.1007/s11434-012-5545-9>
- Kalnay E, Kanamitsu M, Kistler R, Collins W, Deaven D, Gandin L, Iredell M, Saha S, White G, Woollen J, Zhu Y, Leetmaa A, Reynolds R, Chelliah M, Ebisuzaki W, Higgins W, Janowiak J, Mo KC, Ropelewski C, Wang J, Jenne R, Joseph D (1996) The NCEP/NCAR 40-year reanalysis project. *Bull Am Meteorol Soc* 77:437–471. [https://doi.org/10.1175/1520-0477\(1996\)077<0437: TNYRP>2.0.CO;2](https://doi.org/10.1175/1520-0477(1996)077<0437: TNYRP>2.0.CO;2)
- Karl TR, Knight RW (1998) Secular trends of precipitation amount, frequency, and intensity in the United States. *Bull Am Meteorol Soc* 79:231–241. [https://doi.org/10.1175/1520-0477\(1998\)079<0231: STOPAF>2.0.CO;2](https://doi.org/10.1175/1520-0477(1998)079<0231: STOPAF>2.0.CO;2)
- Kemball-Cook S, Wang B (2001) Equatorial waves and air-sea interaction in the boreal summer intraseasonal oscillation. *J Clim* 14:2923–2942. [https://doi.org/10.1175/1520-0442\(2001\)014<2923: EWAASI>2.0.CO;2](https://doi.org/10.1175/1520-0442(2001)014<2923: EWAASI>2.0.CO;2)
- Kikuchi K, Wang B (2009) Global perspective of the quasi-biweekly oscillation. *J Clim* 22:1340–1359. <https://doi.org/10.1175/2008JCLI2368.1>
- Knapp KR, Michael CK, David HL, Howard JD, Neumann CJ (2010) The International Best Track Archive for Climate Stewardship (IBTrACS): unifying tropical cyclone data. *Bull Am Meteorol Soc* 91:363–376. <https://doi.org/10.1175/2009BAMS2755.1>
- Liu G, Wu R (2016) Spatial and temporal characteristics of summer precipitation events spanning different numbers of days over Asia. *Int J Climatol* 36:2288–2302. <https://doi.org/10.1002/joc.4495>
- Liu BH, Xu M, Henderson M, Qi Y (2005) Observed trends of precipitation amount, frequency, and intensity in China, 1960–2000. *J Geophys Res-Atmos* 110:D08103. <https://doi.org/10.1029/2004JD004864>
- Liu Y, Huang G, Huang R (2011) Inter-decadal variability of summer rainfall in eastern China detected by the Lepage test. *Theor Appl Climatol* 106:481–488. <https://doi.org/10.1007/s00704-011-0442-8>
- Liu G, Wu R, Wang H (2016) Contribution of intraseasonal oscillation to long-duration summer precipitation events over southern China. *Atmos Oceanic Sci Lett* 10:82–88. <https://doi.org/10.1080/16742834.2017.1233799>
- Lu E, Zeng YT, Luo YL, Ding Y, Zhao W, Liu SY, Gong LQ, Jiang Y, Jiang ZH, Chen HS (2014) Changes of summer precipitation in China: the dominance of frequency and intensity and linkage with changes in moisture and air temperature. *J Geophys Res-Atmos* 119: 12575–12587. <https://doi.org/10.1002/2014jd022456>
- Lutz AF, Immerzeel WW, Shrestha AB, Bierkens MFP (2014) Consistent increase in high Asia's runoff due to increasing glacier melt and precipitation. *Nat Clim Chang* 4:587–592. <https://doi.org/10.1038/nclimate2237>
- Malik N, Bookhagen B, Mucha PJ (2016) Spatiotemporal patterns and trends of Indian monsoonal rainfall extremes. *Geophys Res Lett* 43: 1710–1717. <https://doi.org/10.1002/2016GL067841>
- Mao J, Chan JCL (2005) Intraseasonal variability of the South China Sea summer monsoon. *J Clim* 18(13):2388–2402. <https://doi.org/10.1175/JCLI3395.1>
- Minářová J, Müller M, Clappier A, Hänsel S, Hoy A, Matschullat J, Kašpar M (2017) Duration, rarity, affected area, and weather types associated with extreme precipitation in the Ore Mountains (Erzgebirge) region, Central Europe. *Int J Climatol* 37:4463–4477. <https://doi.org/10.1002/joc.5100>
- Nguyen P, Thorstensen A, Sorooshian S, Hsu K, Aghakouchak A, Ashouri H, Tran H, Braithwaite D (2018) Global precipitation trends across spatial scales using satellite observations. *Bull Am Meteorol Soc* 99:689–697. <https://doi.org/10.1175/bams-d-17-0065.1>
- Norris J, Chen G, Neelin JD (2019) Changes in frequency of large precipitation accumulations over land in a warming climate from the CESM large ensemble: the roles of moisture, circulation, and duration. *J Clim* 32:5397–5416. <https://doi.org/10.1175/jcli-d-18-0600.1>
- Qian W, Lin X (2005) Regional trends in recent precipitation indices in China. *Meteorol Atmos Phys* 90:193–207. <https://doi.org/10.1007/s00703-004-0101-z>
- Screen JA, Simmonds I (2014) Amplified mid-latitude planetary waves favour particular regional weather extremes. *Nat Clim Chang* 4: 704–709. <https://doi.org/10.1038/nclimate2271>
- Shi YF, Shen YP, Li DL, Zhang GW, Ding YJ, Hu RJ, Kang ES (2003) Discussion on the present climate change from warm-dry to warm-wet in northwest China. *Quat Sci* 23(2):152–164
- Trenberth KE (2011) Changes in precipitation with climate change. *Clim Res* 47:123–138. <https://doi.org/10.3354/cr00953>
- Trepanier J, Tucker C (2018) Event-based climatology of tropical cyclone rainfall in Houston, Texas and Miami, Florida. *Atmosphere* 9:170. <https://doi.org/10.3390/atmos9050170>
- Wang YJ, Yan F (2014) Regional differentiation and decadal change of precipitation in China in 1960–2010. *Prog Geogr* 33(10):1354–1363
- Wen G, Huang G, Tao W, Liu C (2015) Observed trends in light precipitation events over global land during 1961–2010. *Theor Appl Climatol* 125:161–173. <https://doi.org/10.1007/s00704-015-1500-4>
- Wu R, Wen ZP, Yang S, Li YQ (2010) An interdecadal change in southern China summer rainfall around 1992/93. *J Clim* 23(9):2389–2403. <https://doi.org/10.1175/2009JCLI3336.1>
- Wu R, You T, Hu KJ (2019a) What formed the north-south contrasting pattern of summer rainfall changes over eastern China? *Curr Clim Chang Rep* 5:47–62. <https://doi.org/10.1007/s40641-019-00124-z>
- Wu YJ, Ji HX, Wen JH, Wu SY, Xu M, Tagle F, He B, Duan WL, Li JX (2019b) The characteristics of regional heavy precipitation events over eastern monsoon China during 1960–2013. *Glob Planet Chang* 172:414–427. <https://doi.org/10.1016/j.gloplacha.2018.11.001>
- Yan H (1998) Analysis on the weather and climate features and causes of the extraordinary flood disaster over China in 1998 and the relevant meteorological prediction services. *Clim Environ Res* 3:323–334
- Yan Z, Ji J, Ye D (1990) Northern hemispheric summer climatic jump in the 1960s. Part I: precipitation and temperature. *Sci China Ser B* 33: 97–103
- Yao C, Yang S, Qian W, Lin Z, Wen M (2008) Regional summer precipitation events on Asia and their changes in the past decades. *J Geophys Res* 113:D17107. <https://doi.org/10.1029/2007JD009603>
- Yatagai A, Kamiguchi K, Arakawa O, Hamada A, Yasutomi N, Kitoh A (2012) APHRODITE: constructing a long-term daily gridded precipitation dataset for Asia based on a dense network of rain gauges. *Bull Am Meteorol Soc* 93:1401–1415. <https://doi.org/10.1175/bams-d-11-00122.1>
- Yin YH, Wu SH, Chen G (2009) Regional difference of climate trend and abrupt climate change in China during 1961–2006. *J Nat Resour* 24(12):2147–2157

- Yuan F, Chen W, Zhou W (2012) Analysis of the role played by circulation in the persistent precipitation over South China in June 2010. *Adv Atmos Sci* 29:769–781. <https://doi.org/10.1007/s00376-012-2018-7>
- Zhai P, Zhang X, Wan H, Pan X (2005) Trends in total precipitation and frequency of daily precipitation extremes over China. *J Clim* 18: 1096–1108. <https://doi.org/10.1175/JCLI-3318.1>
- Zhu Y, Wang H, Zhou W, Ma J (2010) Recent changes in the summer precipitation pattern in East China and the background circulation. *Clim Dyn* 36:1463–1473. <https://doi.org/10.1007/s00382-010-0852-9>
- Zolina O (2014) Multidecadal trends in the duration of wet spells and associated intensity of precipitation as revealed by a very dense observational German network. *Environ Res Lett* 9:025003. <https://doi.org/10.1088/1748-9326/9/2/025003>
- Zolina O, Simmer C, Kapala A, Gulev S (2005) On the robustness of the estimates of centennial-scale variability in heavy precipitation from station data over Europe. *Geophys Res Lett* 32:L14707. <https://doi.org/10.1029/2005gl023231>
- Zolina O, Simmer C, Gulev SK, Kollet S (2010) Changing structure of European precipitation: longer wet periods leading to more abundant rainfalls. *Geophys Res Lett* 37:L06704. <https://doi.org/10.1029/2010GL042468>
- Zolina O, Simmer C, Belyaev K, Gulev SK, Koltermann P (2013) Changes in the duration of European wet and dry spells during the last 60 years. *J Clim* 26:2022–2047. <https://doi.org/10.1175/jcli-d-11-00498.1>
- Zong Y, Chen X (2000) The 1998 flood on the Yangtze, China. *Nat Hazards* 22:165–185. <https://doi.org/10.1023/A:1008119805106>

Publisher's note Springer Nature remains neutral with regard to jurisdictional claims in published maps and institutional affiliations.